Optical Remote Sensing Techniques Characterize the Properties of Atmospheric Aerosols

Russell Philbrick[a,b,c], Hans Hallen[a], Andrea Wyant[c],
Tim Wright[b], and Michelle Snyder[a]
[a]Physics Department, and [b]Marine, Earth, and Atmospheric Sciences Departments
North Carolina State University, Raleigh, NC 27695
[c]Electrical Engineering Department, The Pennsylvania State University, University Park, PA 16802

ABSTRACT

Several laser remote sensing techniques are used to characterize the properties of aerosols. The various techniques include: backscatter, optical extinction using Raman scatter, and bistatic/multistatic scattering using the polarization ratio of the scattering phase function. The number density, size, and size distribution are obtained under the assumption of spherical scatterers. Other measurements can be used to describe additional properties, such as aerosol type based upon approximate refractive index and detected departure from spherical, when simultaneous measurements at several wavelengths and several angles are analyzed. Examples are shown to demonstrate our present capability to characterize aerosol particles using recently developed techniques.

Keywords: optical scattering, lidar remote sensing, aerosols, trace atmospheric species, bistatic lidar, Raman lidar

1. INTRODUCTION

Laser remote sensing techniques now provide important tools for determining most of the properties of aerosols, including their physical and chemical characteristics. Examples from several data sets are selected to show the types of information contained in the optical scattering signatures. Improvements in our understanding the distribution of aerosols, their sources, and processes controlling their formation and growth are needed for a detail understanding of their contributions to the planetary albedo and their influence on radiative transfer. These are critically important factors for developing accurate predictions of changes to be expected in our climate.

Multi-wavelength backscatter measurements from Rayleigh and Raman lidar techniques provide signals that are used to profile the properties that govern the transmission of radiation through an atmospheric column. Rayleigh lidar signals provide backscatter coefficients, and Raman lidar signals backscattered from the major molecular components provide extinction profiles. The ratio of these simultaneous extinction and backscatter measurements are used to classify the aerosol type. In addition, a laser beam can be used to make bistatic and multistatic measurements of the polarization ratio of the scattering phase function. Analysis of multistatic measurements can be used to determine profiles of the aerosol number density, size, size distribution, and type. These parameters can be determined for spherical particles in the size range between about 20 nm and 20 μm. Analysis of the size distribution requires adopting a mathematical function, which is usually taken to be a log-normal distribution. Information on aerosol type and shape can be supposed from determining the approximate refractive index of the scattering aerosols and by measuring the depolarization of the scattered radiation.

2. RAYLEIGH AND RAMAN SCATTERING

Rayleigh and Raman lidar measurements of scattering by molecules and aerosols provide the profiles of optical backscatter and extinction that determine the atmospheric optical properties influencing radiative transfer. DIAL lidar techniques, hyper-spectral sensors, developments of multi-wavelength lidar, and the recent supercontinuum techniques provide measurements of trace species needed to describe the optical absorption properties that also

Laser Radar Technology and Applications XV, edited by Monte D. Turner, Gary W. Kamerman,
Proc. of SPIE Vol. 7684, 76840J · © 2010 SPIE · CCC code: 0277-786X/10/$18 · doi: 10.1117/12.850453

Downloaded from SPIE Digital Library on 20 May 2010 to 152.1.31.214. Terms of Use: http://spiedl.org/terms

affect the radiation balance. In the troposphere, the direct backscatter optical signals of laser beams from the mixture of molecules and aerosols provides only limited information on the atmospheric properties; primarily they describe cloud ceiling, profiles of relative backscatter coefficient, and indications of the presence of aerosol layers. However, Raman lidar provides more information, including profiles of all major molecular species (N_2, O_2, H_2O), several minor species (O_3, CO_2), temperature, from rotational Raman scattering, dynamical processes, from tracers such as water vapor, and aerosol extinction, from the gradients in the vertical profiles of the molecular constituents [1, 2, 3, 4]. Analyzing the gradients in the vertical profiles of the vibrational Raman signals of N_2, O_2, and the rotational Raman molecular signals, and comparing them with the expected hydrostatic profile of the molecular atmosphere provides robust profiles of the optical extinction at several wavelengths, such as those shown in Fig. 1. The profile of the molecular atmosphere can be obtained using the measured rotational Raman temperature profile. As expected, the profiles of different wavelengths all approach the same value as multiple scattering properties begin to dominate, as in the layer observed at 4.5 km. Extinction profiles for several wavelengths are quite useful for observing changes in the particle size, as a function of altitude and time. In the case of shown in Fig. 1, where different wavelengths are used (284, 530 and 607 nm), we observe changes in time and space for particles in the size range referred to as accumulation mode particles.

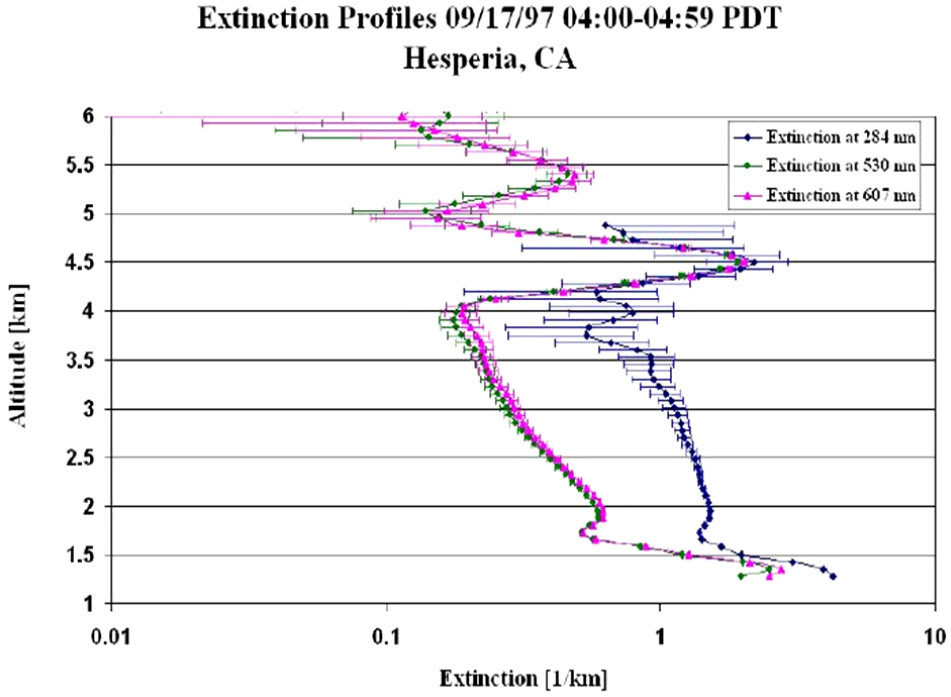

Figure 1. Vertical extinction profiles from gradients in the vibrational Raman profiles of N_2 at 284 and 607 nm, and rotational Raman scattering profiles of the integrated band at 530 nm are shown [4, 5].

Comparison of the ultraviolet and visible wavelength extinction profiles as a function of time in Fig. 2 shows the evolution of cloud development. The time sequence of the 1-minute Raman lidar profiles used to find the gradients from the hydrostatic profile that are caused by the extinction. The vertical profiles are smoothed to provide set of results shown in Fig. 2. The extinction at visible and ultraviolet wavelengths exhibits the fact that the smaller particles are more easily detected at the shorted wavelength. Figure 3 shows water vapor and optical extinction profiles stacked in a time sequence during the early development of a cloud, which is sub-visual in these initial stages. The evolution in a developing cloud is first detected as an increase in the water vapor concentration, and then the aerosols are detected as ultraviolet extinction, and later as extinction at visible wavelengths. Figure 4 presents a time sequence of optical extinction for the ultraviolet and visible wavelengths, where enhanced scattering by smaller particles is observed in the shorter wavelength (UV) plot. The values become comparable within the cloud where multiple scattering dominates, as observed in Fig. 1.

Downloaded from SPIE Digital Library on 20 May 2010 to 152.1.31.214. Terms of Use: http://spiedl.org/terms

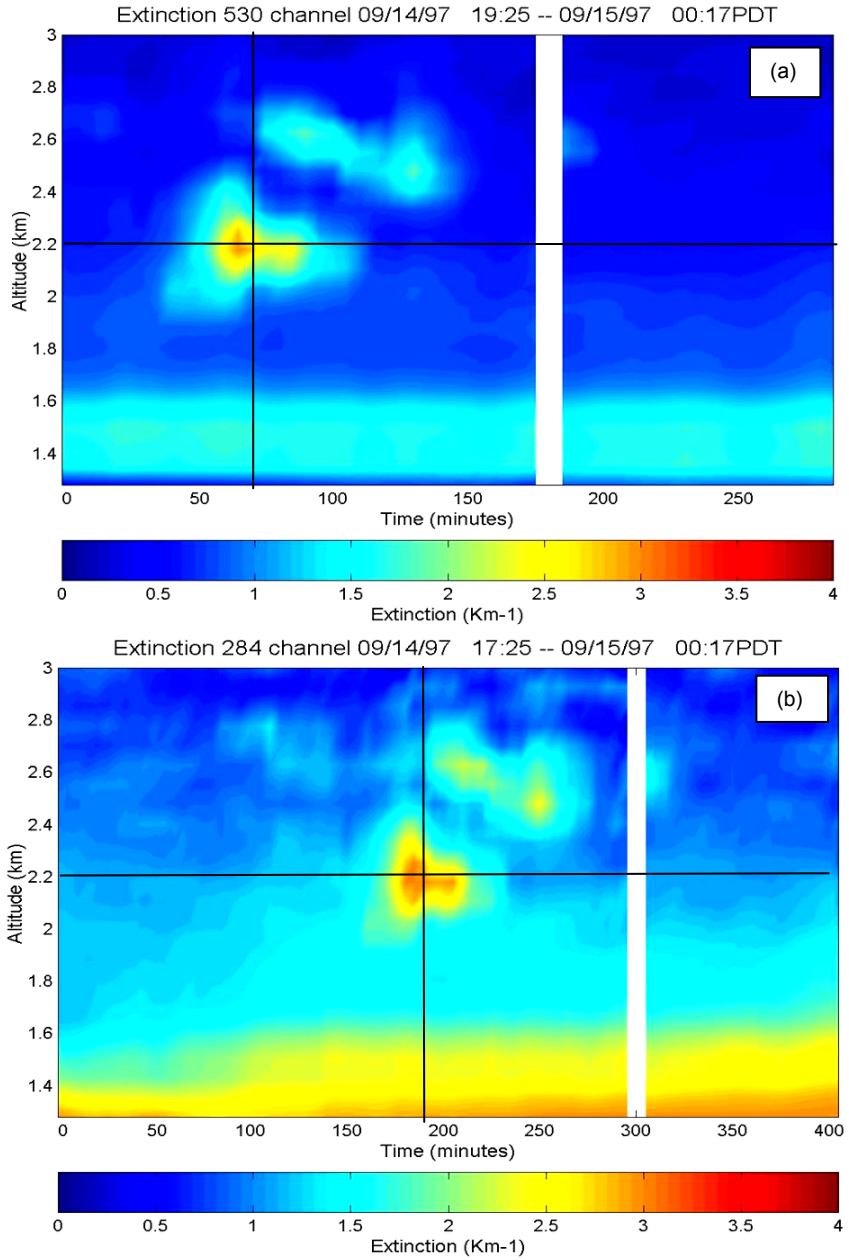

Figure 2. A time sequence of optical extinction profiles shows the development of a cloud moving through the vertical lidar beam; (a) visible (530 nm), (b) ultraviolet (284 nm). Notice that the ultraviolet extinction shows the regions of smaller particles surrounding the thin clouds, as well as the small particle haze layer that was present near the ground. The lines assist in locating an altitude and time point of simultaneous measurements. These measurements were made during the SCOS97 study on 14 September 1997 at Hesperia CA at an elevation of 1.2 km [3, 5].

Downloaded from SPIE Digital Library on 20 May 2010 to 152.1.31.214. Terms of Use: http://spiedl.org/terms

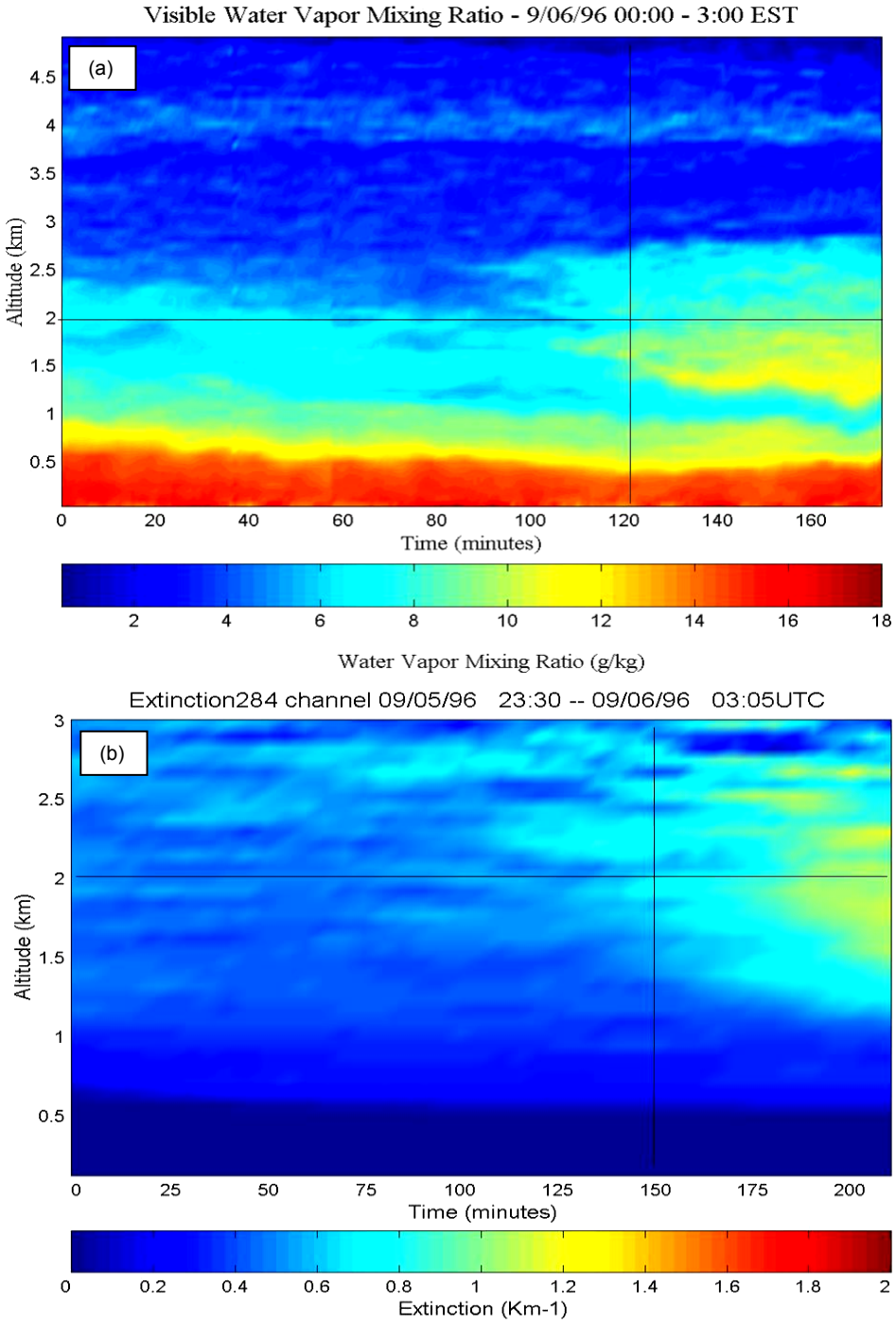

Figure 3. (a) Time sequences of water vapor profiles indicate the development of a cloud occurs before it is evident in the extinction profiles shown in (b); the lines are added to assist in locating corresponding points. [4, 5, 6]

Downloaded from SPIE Digital Library on 20 May 2010 to 152.1.31.214. Terms of Use: http://spiedl.org/terms

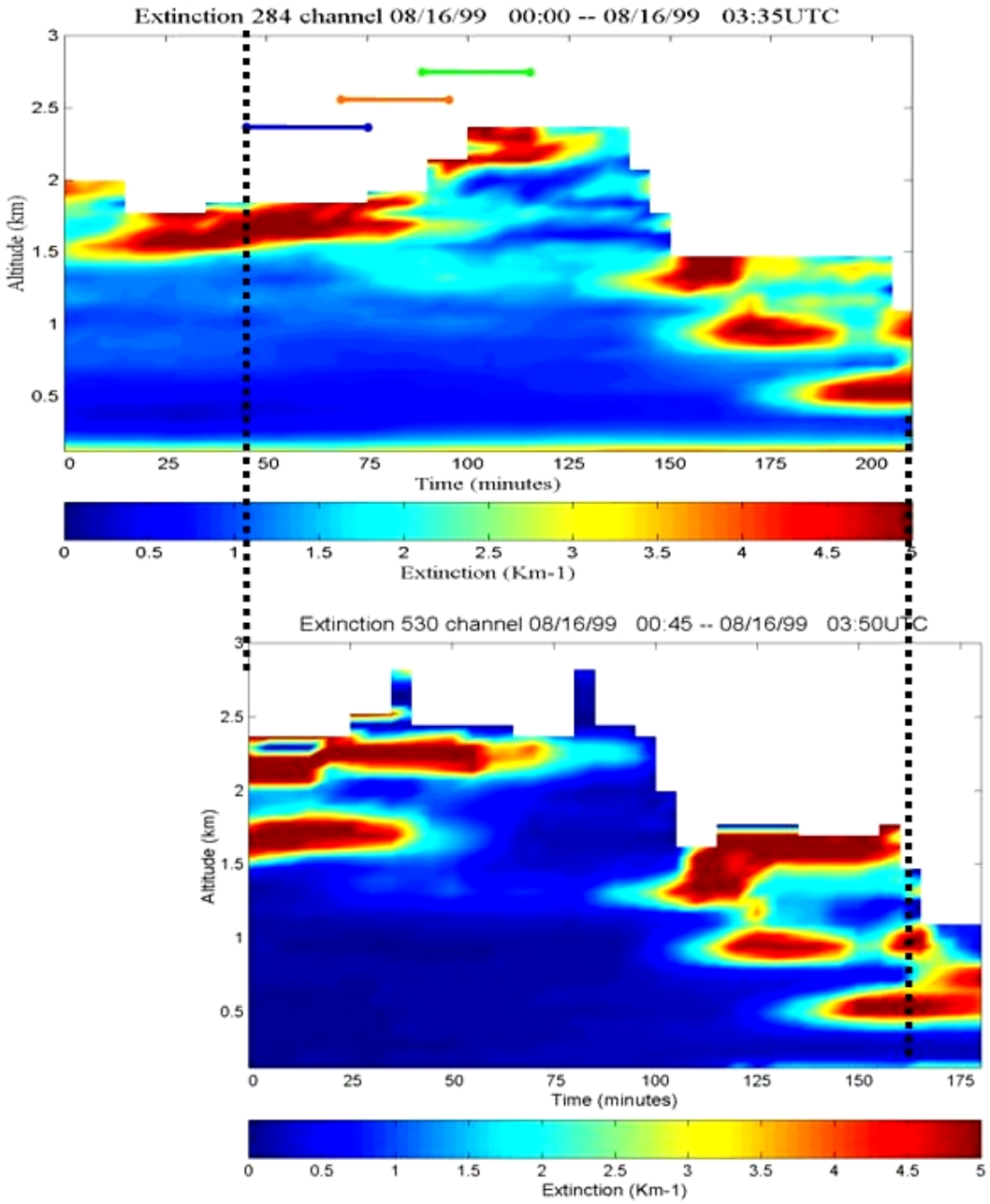

Figure 4. Time sequences of cloud scattering, at ultraviolet (284 nm) and visible (530 nm) wavelengths show the locations of scattering from smaller particles surrounding the clouds [5, 7].

The simultaneous Raman lidar measurements of water vapor and temperature measured during a 6-hour period on the USNS Sumner are shown in the left-hand panels of Fig. 5. These two data sets are used to directly calculate the relative humidity, which is shown in the upper right panel. Comparisons of the measurements of optical extinction in the lower right panel with the relative humidity demonstrate the relationship between the aerosol occurrences and the regions of higher humidity.

Downloaded from SPIE Digital Library on 20 May 2010 to 152.1.31.214. Terms of Use: http://spiedl.org/terms

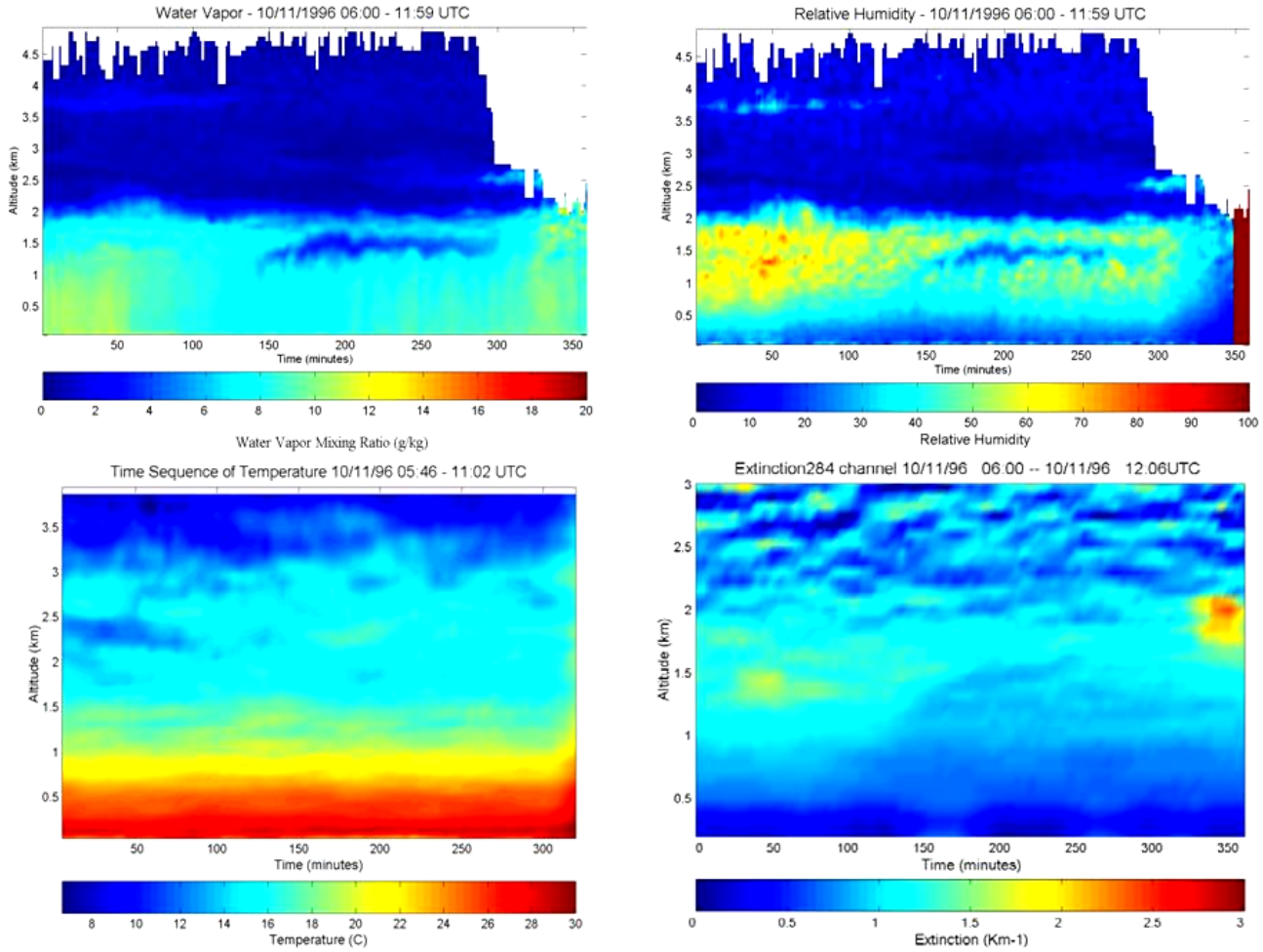

Figure 5. The parameters measured by the Raman lidar, water vapor and temperature (left side) are used to calculate the relative humidity, and this can be compared with the measured extinction to examine the regions of haze and cloud formation [4].

3. AEROSOL SCATTERING

The previous section shows examples that demonstrate that the optical extinction profiles can be obtained directly from the Raman lidar profile measurements of the primary molecular constituents; and additionally information on the changes in particle size can be inferred. The same laser beam that is used for the vertical or horizontal Raman lidar measurements can also be imaged to obtain bistatic lidar data that is analyzed to use the scattering phase function and determine more details regarding the aerosol properties. Figure 6 shows a classic picture of the scattering phase function for two polarization planes, and depicts Mie scattering conditions. These four cases show the angular intensity of the scattered radiation increases and the pattern becomes more complex as the ratio of the particle size to the wavelength increases. The scattering phase function of each polarization of the incident light (perpendicular or parallel with the plane containing the beam and the imaging device) can be measured from digital images of the beam. Investigations using the intensity of the scattering to study aerosol properties was examined earlier [8, 9]; however, our more recent investigations are make use of the information contained in the imaged beam, and make use of the polarization ratio of the scattering phase function to eliminate uncertainties from the extinction along paths between the scattering volume and the imaging detectors. Figures 7, 8, 9, and 10 show results from a series of tests designed to demonstrate this capability by using bistatic lidar measurements to describe aerosol properties.

Downloaded from SPIE Digital Library on 20 May 2010 to 152.1.31.214. Terms of Use: http://spiedl.org/terms

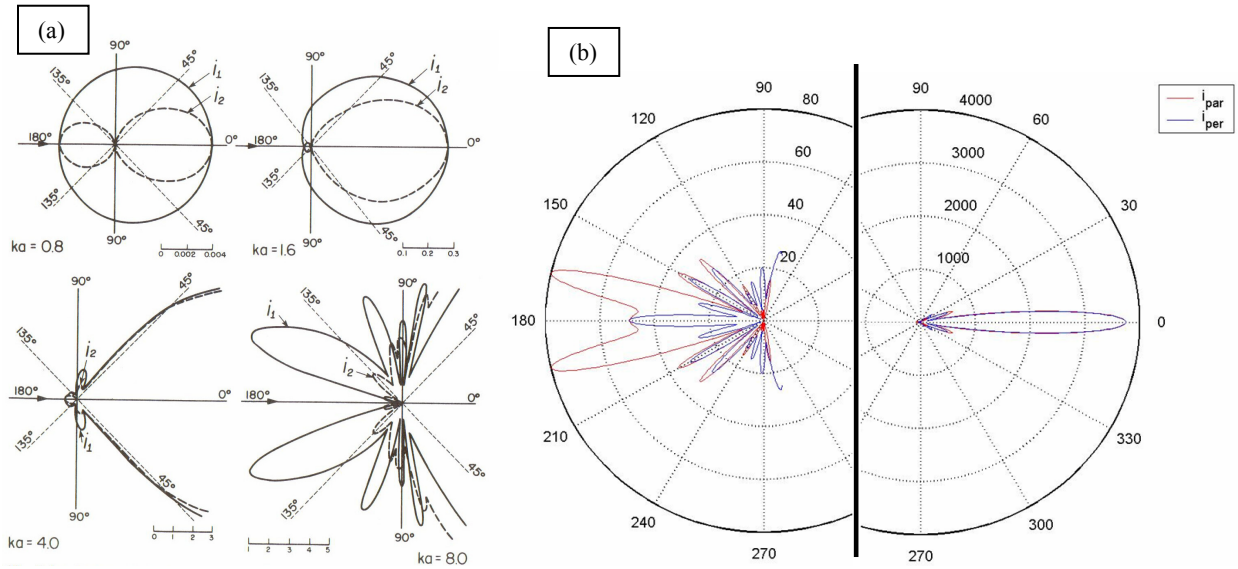

Figure 6. (a) The angular variation of the intensity of the scattering phase function is shown for both polarizations and several cases of $k = 2\pi a/\lambda$ (a is the particle size and λ is the scattering wavelength [10]; (b) polar plot of the scattering phase function for the two polarization components is shown for the case of 1 μm diameter particles illuminated with 500 nm wavelength laser beam, and the rhs shows a magnified scale of the backscatter intensity [11, 12].

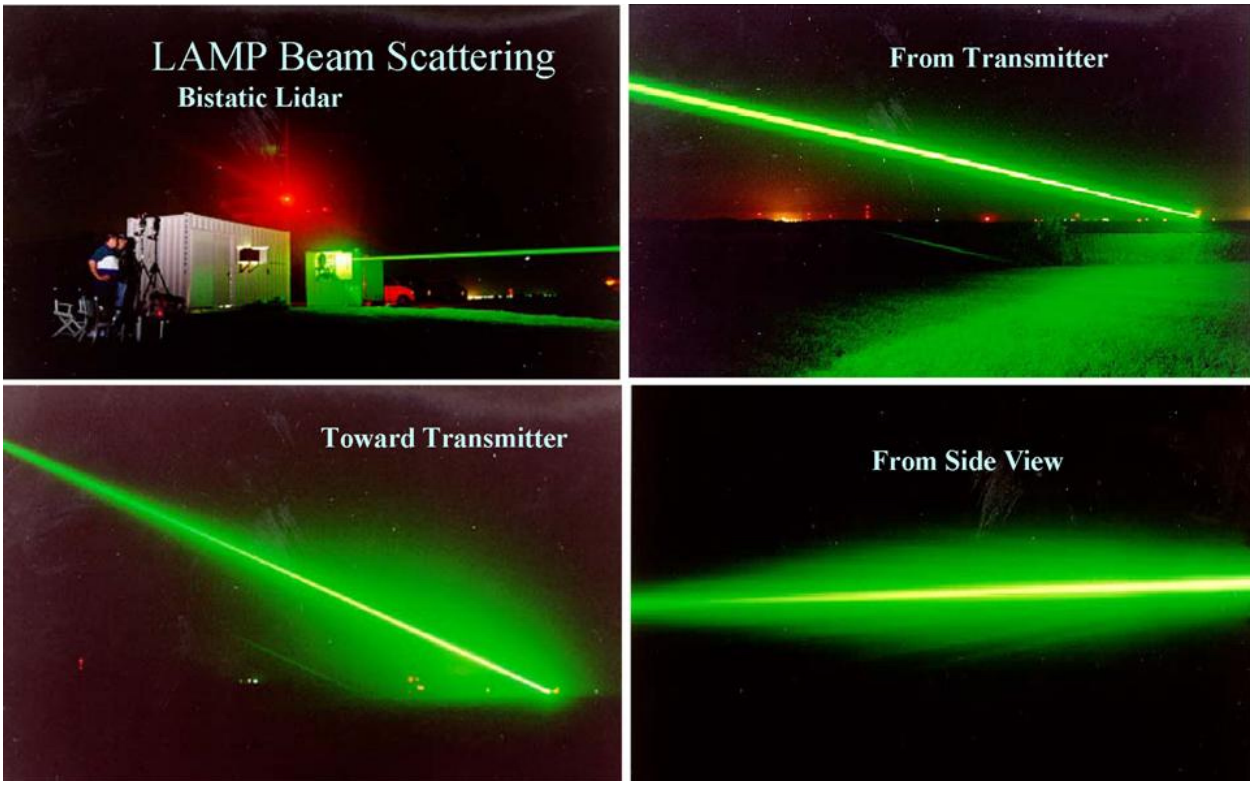

Figure 7. Photographs of a laser beam propagating through a haze that developed during a night with radiation fog (Philbrick). The views of the arrangement in Fig.7, looking along the beam, back toward the transmitter, and from the side show the classic intensity distributions from the scattered intensity.

Downloaded from SPIE Digital Library on 20 May 2010 to 152.1.31.214. Terms of Use: http://spiedl.org/terms

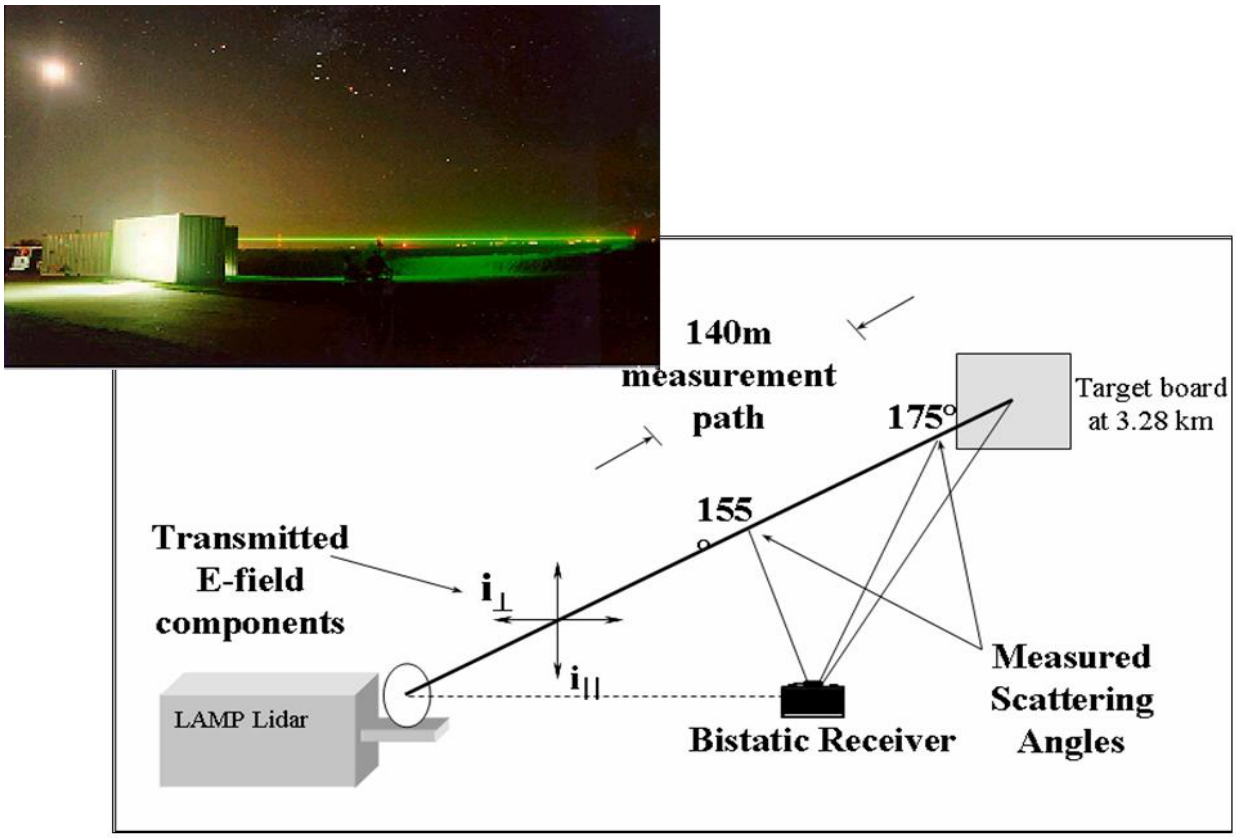

Figure 8. Arrangement used for the bistatic lidar measurements during the CASES project at NASA Wallops in September 1995. The measurements were made using the LAMP Raman lidar which measured optical extinction on the path [13, 14].

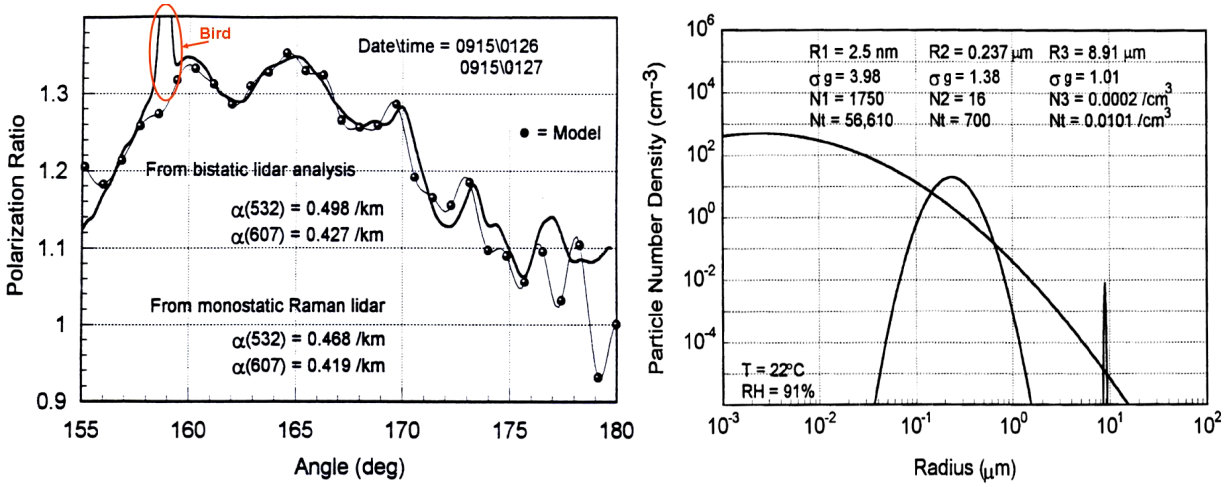

Figure 9. (a) Polarization ratio from the measured intensities is compared with calculations from the best fit solutions of the Mie equations; (b) the solution for the results in (a) are shown for fitting these tri-modal distributions to determine the density and size (peak and distribution width) -- the peak at 9 μm contributes most to scattering [13, 14, 15].

Our approach for most bistatic measurements is to make use of the high power Raman lidar beam. Research campaigns have used horizontal paths with end-points on hard targets, like the one shown in Fig. 8, and vertical measurements using several receivers to resolve layered structures. Vertical measurements of the Raman lidar provide an ideal configuration for making multi-static measurements of the aerosol properties. It was found that vertical measurements require

Downloaded from SPIE Digital Library on 20 May 2010 to 152.1.31.214. Terms of Use: http://spiedl.org/terms

simultaneous data at two or more angles to resolve the aerosol properties. The system uses imaging detectors to measure the intensity as a function of angle, and the detectors are placed along radials on the planes of the parallel and perpendicular polarization of the laser transmitter. If one radial is used, the polarization plane can be flipped 90^o by inserting a polarization rotator. Measurements of the two components of polarization are normally obtained within a period of a few seconds (optical shutter times are a fraction of a second to a couple of seconds), and data sets are typically obtained in a sequence at a rate of about once per minute.

An example from the bistatic measurements and analysis results from the CASES experiment is shown in Fig. 9. In Fig. 9(a), the polarization ratio formed from the intensities of each pixel interval in the imaging array is plotted versus angle. The data for angles near 180^o does not contain significant information. The analysis uses an array calculated from the Mie equations of aerosol scattering for spherical particles to find the best match for a tri-modal distribution of particles. The free parameters to be fit are the size and distribution of sizes, and the number densities for the three modes. The polarization ratio from the best fit solution for this particular case are plotted as points along with the measurements in Fig. 9(a). In addition to the assumption of spherical particles, an assumption for the size distribution function is necessary; we have selected the log-normal distribution. Another parameter that can be estimated from the analysis is the index of refraction. Figure 9(b) shows the solution for data in Fig. 9(a). The best fit parameters for this case are shown in the top of Fig. 9(b). The integrated extinction that would be caused by the scattering particles can be calculated for any wavelength using the values for the density, size, size distribution and index of refraction of the particles. The optical extinction values at 532 and 607 nm corresponding to the solution in Fig. 9(b) are printed in the inset of Fig. 9(a). The values obtained from the Raman lidar measurements obtained at the same time are also given. The extinction values differ by about 5% and are within the measurement errors.

4. MULTISTATIC SENSING OF AEROSOLS

The developments of the analysis of vertical profiles requited a different approach to resolve the profiles of the vertical structure through the often present aerosol layers. The key to obtaining accurate results is to over-determine the solution by making measurements at several different angles simultaneously in overlapping the field-of-view (fov) from several imagers; four or five locations along the radial are preferred. The angles can be determined accurately in the case when the end-point of the vertical beam is contained in the fov; also the star field can be imaged at night. The imagers are fitted with band filters for the laser wavelength (532 nm was used in this case), but the bandwidth cannot be narrow or the angular acceptance is too small. Future configurations will make use of confocal optics to allow use of narrow band filters and permit measurements in higher backgrounds. Figure 10 shows the arrangement that was used to acquire the multistatic lidar measurements [11, 12]. Experience has indicated that three to five images are needed to provide sufficient resolution in regions where the change on the aerosol density is changing rapidly with height. The simultaneous measurements of each pixel height provide the possibility to remove the ambiguity in the solution. Figure 11 shows a data set that was obtained for a low altitude layer of aerosols. Figure 12 is an example of an analyzed data set that was fit with a bi-modal size distribution.

The initial development of the bistatic lidar technique that images an angular range of the scattering from a laser beam and uses the polarization ratio of the scattering phase function to analyze the results was accomplished by Stevens [13, 14, 15]. A major advance in our use of the scattering information resulted from the work of Novitsky [11, 12], when he developed the multistatic lidar system. The technique has been extended to the case of aerosol multiple scattering and resulted in useful experimental and theoretical advances [16, 17]. A solution for the full range of angles of scattering phase function for the case of multiple scattering is now available; previously, the regions near 0^o and 180^o were available. The next advances are underway by making use of multi-wavelength scattering using several laser wavelengths simultaneously; even the case of using a supercontinuum laser is studied [18]. The investigations of aerosols are being combined with measurements of other meteorological parameters from Raman lidar and from Differential Absorption Spectroscopy (DAS) to examine the optical properties through the optical spectrum [19, 20].

Downloaded from SPIE Digital Library on 20 May 2010 to 152.1.31.214. Terms of Use: http://spiedl.org/terms

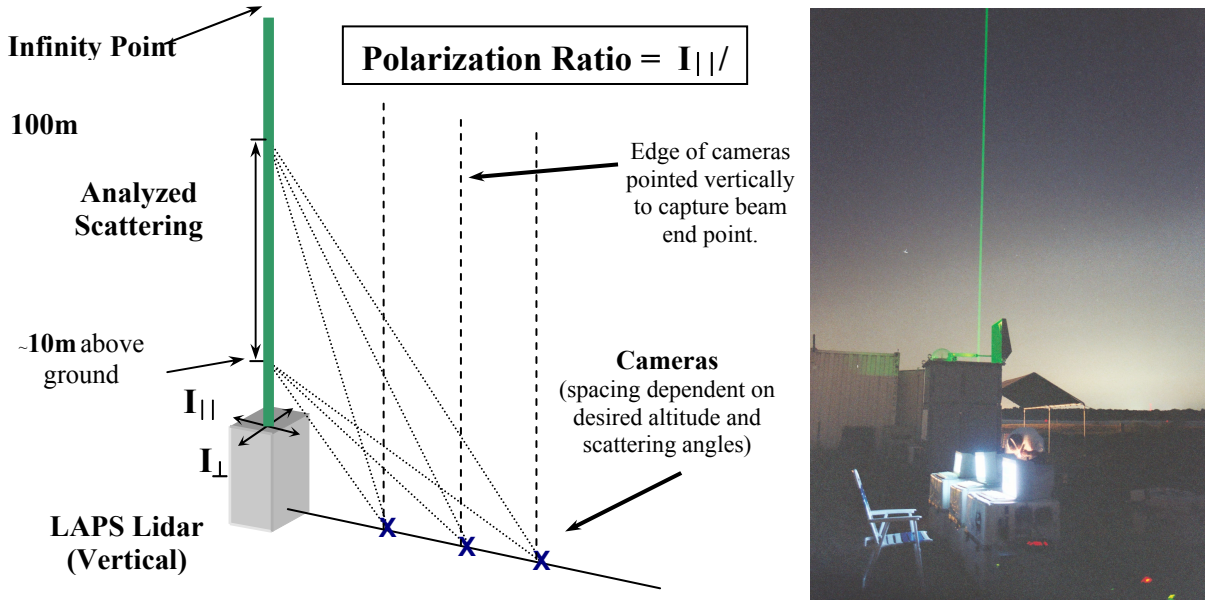

Figure 10. The arrangement for the multistatic lidar measurements is shown [12].

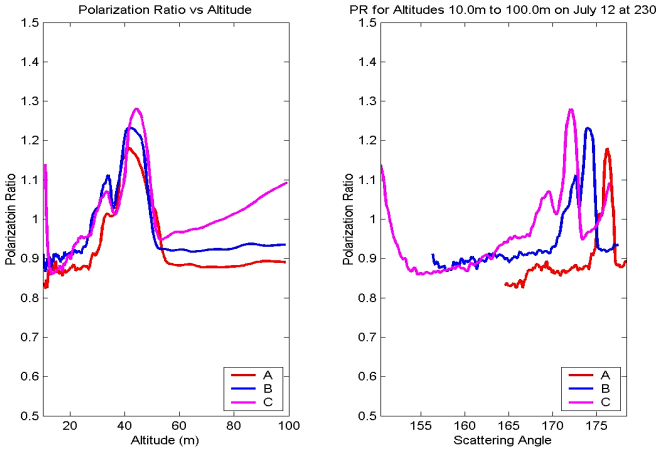

Figure 11. A low altitude aerosol layer is investigated with the multistatic lidar. The figures show the polarization ratio plotted versus altitude and scattering angle to see the difference [11, 12].

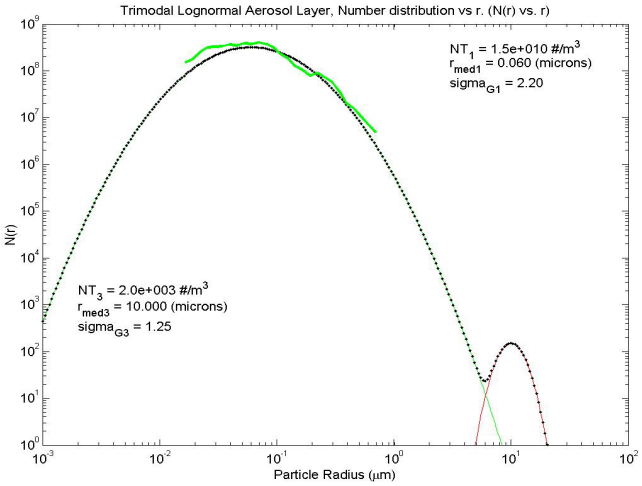

Figure 12. Analysis of this particular multistatic lidar data was best fit with a bi-modal size distribution with 60 nm and 10 μm particle size distributions [11, 12].

Downloaded from SPIE Digital Library on 20 May 2010 to 152.1.31.214. Terms of Use: http://spiedl.org/terms

5. REFERENCES

[1] O'Brien, M.D. T. D. Stevens and C. R. Philbrick, "Optical Extinction from Raman Lidar Measurements," Optical Instruments for Weather Forecasting, SPIE Proc. 2832, 45-52 (1996).

[2] Philbrick, C.R., "Raman Lidar Descriptions of Lower Atmosphere Processes," Lidar Remote Sensing in Atmospheric and Earth Sciences, Proc. 21st ILRC, Valcartier, Quebec Canada, 535-545 (2002).

[3] Li, Guankun, and C. Russell Philbrick, "Lidar Measurements of Airborne Particulate Matter," in Remote Sensing of the Atmosphere, Environment, and Space, SPIE , 4893-15 (2002).

[4] Philbrick, C.R., "Raman Lidar Characterization of the Meteorological, Electromagnetic and Electro-optical Environment," Proc. SPIE Vol. 5887, Lidar Remote Sensing for Environmental Monitoring VI, p. 85-99 (2005).

[5] Verghese, Sachin J., Adam H. Willitsford and C. Russell Philbrick, "Raman Lidar Measurements of Aerosol Distribution and Cloud Properties," Lidar Remote Sensing for Environmental Monitoring VI, edited by Upendra N. Singh, Proc. of SPIE Vol. 5887 H-1 (2005).

[6] Philbrick, C. Russell, "Overview of Raman Lidar Techniques for Air Pollution Measurements," Lidar Remote Sensing for Industry and Environment Monitoring II, SPIE , 136-150 (2002).

[7] Verghese, Sachin, [PhD Dissertation], Department of Electrical Engineering, Penn State University (2008).

[8] Reagan, J.A., D.M. Byrne and B.M. Herman, "Bistatic LIDAR: A Tool for Characterizing Atmospheric Particulates: Part I – The Remote Sensing Problem," IEEE Geosciences and Remote Sensing 20, 229 (1982a).

[9] Reagan, J.A., D.M. Byrne and B.M. Herman, "Bistatic LIDAR: A Tool for Characterizing Atmospheric Particulates: Part II – The Inverse Problem," IEEE Geosciences and Remote Sensing 20, 236 (1982b).

[10] Born, Max and Emil Wolf, [Principles of Optics] Cambridge University Press, New York (2002).

[11] Novitsky, E. J., and C.R. Philbrick, "Multistatic Lidar Profiling of Urban Atmospheric Aerosols," J. Geophy. Res. - Atmospheres, 110, DO7S11 (2005).

[12] Novitsky, Edward J., [PhD Dissertation], Department of Electrical Engineering, Penn State University (2002).

[13] Stevens, T.D., and C. R. Philbrick, "Particle Size Distributions and Extinction Determined by a Unique Bistatic Lidar Technique," Proceeding of IGARSS96 Conference on Remote Sensing for a Sustainable Future (International Geophysics and Remote Sensing Symposium) II, 1253-1256 (1996a).

[14] Stevens, T.D., and C. R. Philbrick, "A Bistatic Lidar Receiver to Observe Lower Tropospheric Aerosol Properties," Proceedings of the 18th Annual Conference on Atmospheric Transmission Models, 6-8 June 1995, PL-TR-96-2080, Special Report 278, Phillips Laboratory, Hanscom AFB MA 01731, 242, (1996b).

[15] Stevens, Timothy D., [PhD Dissertation], Department of Electrical Engineering, Penn State University (1996).

[16] Park, Jin H., and C. Russell Philbrick, "Multiple Scattering Measurements Using Multistatic Lidar," Proc. International Aerosol Conference (2006).

[17] Park, Jin H., PhD Dissertation, Department of Electrical Engineering, Penn State University, 2008.

[18] Wyant, Andrea M., David M. Brown, Perry S. Edwards, and C. Russell Philbrick, "Multi-wavelength, multi-angular lidar for aerosol characterization" Laser Radar Technology and Applications XIV, Proc. of SPIE Vol. 7323 (2009)

[19] Philbrick, C. Russell, David M. Brown, Adam H. Willitsford, Perry S. Edwards, Andrea M. Wyant, Zhiwen Z. Liu, C. Todd Chadwick, and Hans Hallen, "Remote Sensing of Chemical Species in the Atmosphere" *Proc. of Fourth Symposium on Lidar Atmospheric Applications*, as part of the 89th AMS Annual Meeting (2009) http://ams.confex.com/ams/pdfpapers/150051.pdf

[20] Philbrick, C. Russell, Hans Hallen, "Measurements of Contributors to Atmospheric Climate Change," Proc. 19th Symposium on European Rocket and Related Research, ESA Special Publication SP-671 (2009).

Downloaded from SPIE Digital Library on 20 May 2010 to 152.1.31.214. Terms of Use: http://spiedl.org/terms